

Energy Dissipation Capacity of Columns and the Time of Collapse of Steel Structures

K.S.Sivakumaran

*Department of Civil Engineering, McMaster University, Hamilton, Ontario, Canada L8S 4L7
siva@mcmaster.ca*

R.M. Korol

*Department of Civil Engineering, McMaster University, Hamilton, Ontario, Canada L8S 4L7
korol@mcmaster.ca*

Abstract

Steel buildings subjected to excessive gravity loads, such as debris pile up caused by controlled demolitions, fire or other extreme events, may suffer partial or complete collapse. This paper investigates the influence of the energy dissipation capacity of columns on the time of complete collapse or arrested collapse. The first part of the paper discusses a recent test program that deals with the energy dissipation capacity of square steel box sections subjected to continuous axial loading. Eleven hollow structural steel specimens were tested quasi-statically and they primarily exhibited crush progression of inward and outward folds propagating over the length. These tests suggest that hollow squares are much more desirable as columns than open sections in such circumstances. The second part of the paper employs Newton's laws of motion to predict the velocity profiles and time of the collapse of multi-storey buildings undergoing gravity induced progressive collapse. A formulation of the problem of a building frame of "N" stories, subjected only to gravity loading is postulated that involves an analysis employing a generic one-dimensional discrete model of progressive collapse. An example 10-storey structure is considered to illustrate the method. For the design scenarios postulated, major differences in collapse times were found. Many of the cases considered resulted in collapse arrest of the building at some intermediate floor level.

Keywords

Multi-storey steel building, Progressive collapse, Collapse time, Hollow-square columns, Energy dissipation capacity

1. Introduction

The progression and the time of collapse of structures has not been a topic of significant interest of the structural engineering profession. However, these parameters, which depend primarily on the energy dissipation capacities of the columns, are of importance during excessive gravity loads (debris pile up) induced failures, total or partial collapse, due to events such as controlled demolitions or fire. The objective of this paper is to examine gravity load induced progressive collapse of multi-storey steel buildings by employing the most basic equations of Newton's laws of motion and equations of energy and momentum. First part of the paper discusses the energy dissipation capacity of square hollow structural steel box sections. The second part of the paper considers the velocity profiles and time of collapse of a multi-storey building undergoing gravity induced progressive collapse.

2. Energy Dissipating Capacity of Columns

The steel columns of a building can fail in various ways, which can lead to a total building collapse. A three plastic hinged buckling mode failure assumption may be reasonable for wide flange columns that are rigidly supported at upper and lower floor levels. A single plastic hinge at the mid-height energy dissipation model may be appropriate for columns that are poorly supported at upper and lower floor levels. However, when square tubular members are employed, that are rigidly supported at each floor level, the effective slenderness ratios are generally significantly reduced. Such short to intermediate columns fail in axial crushing, which is an efficient energy dissipating failure mode.

This section summarizes the tests recently undertaken at McMaster University to establish the energy absorption of square Hollow Structural Section (HSS) steel columns in the short to intermediate range subjected to axial crush forces. A total of eleven square HSS specimens (Grade 350 Class H), the specified outer dimensions of which were 101.6, 127.0 and 152.4 mm, with thicknesses either 4.78 or 6.35 mm and lengths 457 mm to 914 mm were tested. The above lengths coupled with the above cross-sectional properties resulted in effective slenderness parameter λ (See Table 1 Column 2) ranging between 0.15 and 0.20, values which are typically encountered in building applications.

Figure 1 shows the test setup and specimen 125-6-740 during a test. The specimen identification indicates the width-thickness-length dimensions of the specimen. Two string-type LVDTs were employed on opposite sides of the specimen attached to the top and bottom platens to measure the axial shortening. In these tests, typically the local buckling failure was initiated near the top of the box column, followed by folding of the sides as evident from the Figure 1. The axial crush failure mode can be described as beginning from a set of symmetric inward and outward local buckles around the perimeter, that progressed to a state of fully closed loops, followed by axial bearing that caused a secondary rise in load resistance until formation of a second fold pattern, and so on, until the entire section would potentially be an array of in and out folds. The resulting load-displacement curve is also shown in Figure 1.

Table 1 summarizes the test results. The cross-sectional area of these columns varied between 1790 mm² and 2960 mm². Tension coupon tests established the yield strengths, which ranged between 366 MPa and 484 MPa. The axial yield load $P_y = \sigma_y A$, where σ_y is the measured yield stress, ranged between 655 kN and 1433 kN. Table 1 shows the peak loads attained during these tests, which is highlighted in Figure 1 as P_{max} , and they ranged between 769 kN and 1728 kN. The yield loads are widely used in design codes. Evidently, the ultimate loads were higher than the yield loads. On average, they were 17% higher, which may be attributable to strain hardening effects. Tests were terminated after the specimens had fully folded with the maximum recorded axial shortening shown in Table 1 and in Figure 1 as Δ_{max} . The energy absorbed as noted in both the table and the figure is the area under the load-displacement curve for that particular specimen up to its maximum displacement value Δ_{max} . By dividing the energy by the total displacement Δ_{max} an average resistance value P_{avg} was computed, which is shown in column 7 of Table 1.

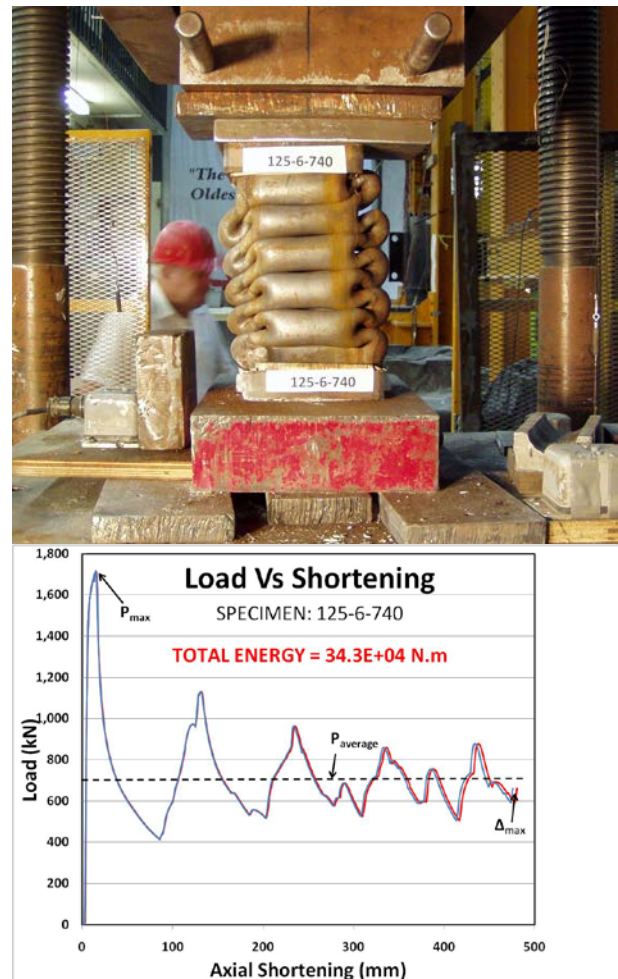


Figure 1: Crush Test Specimen 125-6-740

Table 1: Square Tubular Columns Subjected to Axial Compression

Specimen	$\lambda = KL/t$ [$\sqrt{(F_y/\pi^2 E)}$]	P_y (kN)	P_{max} (kN)	Δ_{max} (mm)	Energy (N.m)	P_{avg} (kN)	P_m (kN)	P_{avg}/P_m
(1)	(2)	(3)	(4)	(5)	(6)	(7)	(8)	(9)
100-5-590	0.20	655	774	241	7.91E+04	328	212	1.54
100-5-510	0.17	655	773	334	1.11E+05	332	212	1.60
100-5-440	0.15	655	769	245	7.72E+04	315	212	1.50
100-6-580	0.20	988	1219	119	5.93E+04	498	340	1.46
100-6-430	0.15	988	1246	245	1.54E+05	629	340	1.84
125-5-740	0.20	919	999	435	1.51E+05	347	228	1.50
125-5-560	0.15	919	1000	342	1.18E+05	345	228	1.47
125-6-740	0.20	1433	1718	481	3.43E+05	713	366	1.95
125-6-550	0.15	1433	1728	344	2.45E+05	712	366	1.92
150-5-890	0.20	941	1053	262	9.61E+04	367	242	1.53
150-5-670	0.15	941	1050	396	1.29E+05	326	242	1.34

When compared with the maximum load P_{max} , the average load P_{avg} was considerably lower and ranges from a low of 31% (150-5-670) to a high of 50% (100-6-430). As noted in Table 1, however, the slenderness factor λ , which reflects the slenderness of the member, for these two specimens were equal, i.e. 0.15. For other cases involving the same cross section, the slenderness factor seemingly played only a minor role in determining P_{avg}/P_{max} ratios as well.

As presented in the next section, the sample building considered utilizes square columns, for which the slenderness values were considered to be at the very low end of the cut-off value for short to intermediate length columns and hence such compression members could qualify as short columns, prone to axial crushing. As such an analysis based on tubular crushing may be appropriate when the tubular dimensions and effective lengths warrant it. Research done by Wierzbicki and Abramowicz (1983) and later by Abramowicz and Jones (1986) on both quasi-static and dynamic crushing of tubular members, respectively, is deemed to have relevance in estimating the energy dissipation of such columns during a story collapse event. From their analytical and experimental study, a formula was developed by Wierzbicki and Abramowicz (1983) for the average crushing resistance, P_m , during which progressive stages of plate element folding, compressing, and sequential propagation occurred, until the member became totally squashed. The average crushing resistance, P_m is given as: $P_m = 9.56 \sigma_y t^{5/3} c^{1/3}$, where t and c represent thickness, and outer plate width dimensions, respectively, for squares, with σ_y being the yield stress. Table 1, column 8 shows the corresponding P_m values for the hollow structural sections under consideration, based on $\sigma_y = 350$ MPa. The P_{avg} values established during the current tests are 34-95% higher than the P_m values given by Wierzbicki and Abramowicz (1983). In reality, a collapsing building frame may be subject to high levels of strain rate, thereby having the effect of raising the value of P_m which was based on static tests. Although the current steel box column experiments exhibited somewhat higher crush strength values than is given by P_m , in the analysis presented in the next section, we opted to utilize the expression $(9.56 \sigma_y t^{5/3} c^{1/3})$, due to the limited number of tests considered in this study and for reasons both of simplicity and conservatism. Accordingly, the energy dissipation in each such tubular column in a storey having a height h_i can be established as;

$$ED = [9.56 \sigma_y t_i^{5/3} c_i^{1/3}] h_i \quad (1)$$

where, ED is the energy dissipation potential of a square tubular column, σ_y is the yield stress, t_i and c_i are thickness and outer plate width dimensions of a HSS steel column at story i , respectively, while h_i represents the corresponding height of the crushing displacement. The energy dissipation of stories with multiple tubular columns can then be established by summing the dissipation capacity of each one.

3. An Analysis Model for the Progressive Collapse of a Building

Consider a typical N -story building of height H with square floor and roof dimensions of A as shown in Figure 2. Height h_i is the clear floor height at story i . The mass at floor level i is designated to be m_i . It is postulated that a given story $n \leq N$ is suddenly degraded to a state of zero resistance due to some catastrophic event occurring in story n . The result is a commencement of freefall of the rigid block above story n , until it impacts the floor below (level $n-1$). A sudden reduction in velocity is then expected due to the mass of the rigid block impacting the mass at level $(n-1)$. While the consequent impulse, $F \Delta t$, occurring during the collision gives rise to a short interval of time, its estimation is beyond the scope of this study. Assuming the resulting dynamic impact force exceeds the elastic limit of the resisting columns, plastic deformation occurs and the impact continues to crush the columns in the floor below until either the motion is stopped due to high energy dissipation in that story, or to continue with subsequent collision with the floor below (crush-down collapse). Depending on the mass of the moving crush-down front, its velocity, and the energy dissipation capacity of the columns, the crush-down front may be arrested or it may reach the ground level. If it reaches the ground level, then the columns in floors above level n may begin to collapse, with the front moving upwards (crush-up collapse), until it is arrested or the roof mass comes to rest at the top of the debris pile.

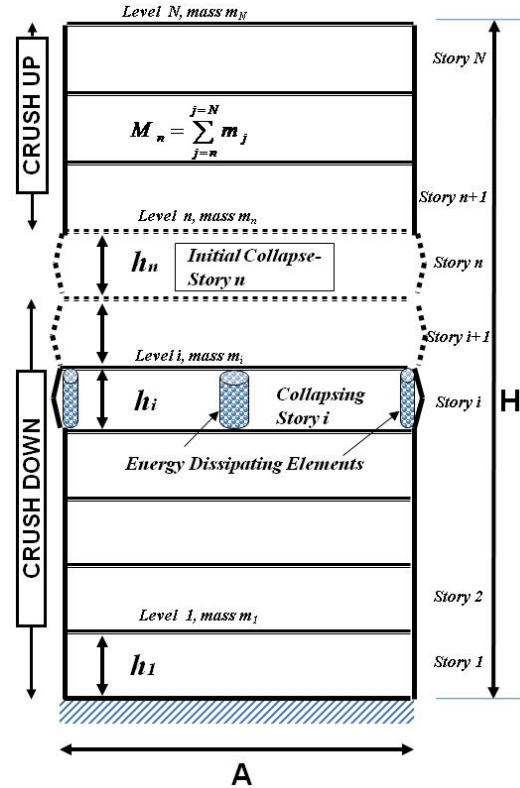


Figure 2: Collapse Analysis Model

Initial Free Fall: When a given story n suddenly collapses, a freefall motion of the stories above level n through height h_n ensues. The stories above the initial collapse story n are intact and freefalling as a rigid body and the total mass of that part of the building may be given as M_n (defined in Figure 2). Considering the motions of a freefalling object, the velocity of this body of mass at impact with the floor below (floor level $n-1$) is given as $V_n^F = \sqrt{2gh_n}$, where g is the gravitational acceleration.

Crush- Down Collapse: Consider the crush-down collapse of the i^{th} story, where $i < n$. Since the stories above level i to level n have already collapsed and the block above the initial collapse story n is intact but freefalling, the total mass falling onto the i^{th} level may be given as M_{i+1} (defined below). The corresponding velocity at impact is designated herein as V_{i+1}^F . Immediately thereafter, the velocity of crush-down is reduced due to the addition of floor mass m_i . The initial velocity of the combined mass given as V_i^I may be obtained through the conservation of linear momentum equation as:

$$[M_{i+1} + m_i]V_i^I = [M_{i+1}]V_{i+1}^F, \quad \text{where } M_{i+1} = \sum_{j=i+1}^{j=N} m_j \quad (2)$$

Assuming the crush-down front propagates through story i , the final velocity V_i^F of the total mass (before impact with floor $i-1$) can be obtained through energy balance involving kinetic, potential and dissipation energy terms for crushing of the i^{th} story as:

$$\frac{1}{2}[M_{i+1} + m_i](V_i^F)^2 = \frac{1}{2}[M_{i+1} + m_i](V_i^I)^2 + [M_{i+1} + m_i]g h_i - ED_i \quad (3)$$

ED_i = the total energy dissipated by such columns in story i , while h_i represents the height of the crushing displacement within storey i , understood as being less than the full story height. An imaginary solution for V_i^F would indicate an arrest of collapse.

Crush-Up Collapse: If the crush-down front reaches the ground floor, then crush-up failures of stories i from $(n + 1)$ to N are likely to occur sequentially. Since subsequent collisions of story masses immediately above story n will occur with the rubble pile (assumed rigid), there will be no velocity loss at impact. As such, the initial velocity for crushing story $n+1$, namely, V_{n+1}^I , will be equal to V_{n+1}^F . Similarly, the initial velocity of crush-up story i , namely V_i^I will be equal to the final velocity of the story below, i.e. V_{i-1}^F . The energy balance can then be applied to compute V_i^F as;

$$\frac{1}{2}[M_i](V_i^F)^2 = \frac{1}{2}[M_i](V_i^I)^2 + [M_i]g h_i - ED_i, \quad \text{where} \quad M_i = \sum_{j=i}^{j=N} m_j \quad (4)$$

M_i is the total mass of the floors above story i , while ED_i is the total energy dissipated by such elements in story i . The calculation is repeated until finally the roof mass m_N comes to rest at the top of the debris pile (total collapse of the structure), or until a partial crush-up failure occurs, indicated by an imaginary final velocity V_i^F of a collapsing story i . As a matter of fact, as explained in the next section, in the event of collapse arrest the height of partially collapse story i can be established by assigning $V_i^F = 0$.

4. Example: Progressive Collapse of a 10-Story Building

This example considers a 10-story building structure with a square plan dimension of $A = 16$ m. Each story is presumed to be of height 4.10 m, with a clear floor to ceiling height of 3.75 m. The building is assumed to be subjected to a dead load of 5.75 kPa, a live load of 3.0 kPa and lateral loads. The mass of the floor was taken as the unfactored dead load of 5.75 kPa, while the live load, devoid of occupants, was limited to $1/3^{\text{rd}}$ the 1.00 kPa value, thus giving a total value of 6.75 kPa. The mass, m_i per floor and roof level (made equal for simplicity), therefore computes as $[6.75 \times (16)^2 \times 1000] / 9.81 = 176,147$ kg. It is assumed that the building consists of four lines of columns. Figure 3 illustrates such a layout. Only the hollow structural tubular columns are considered to be energy dissipation elements and the roof and floor systems are not. In all our cases, it is assumed that the floor system is rigidly connected to the continuous columns, thus providing column end fixity. All tubular steel sections under consideration are assumed to be 350 class H, which provides for a minimal degree of residual stresses from manufacturing (H = hot formed), while the yield stress, σ_y , is 350 MPa. The various column sizes selected are considered as being representative of the building, whose design considered the load combinations arising due to dead, live, wind or earthquake loads consistent with the Load and Resistance Factor Design codes (CSA, 2009). For design and construction convenience the column sections were changed every two floors, however, each story column was designed as pin-pin ended column.

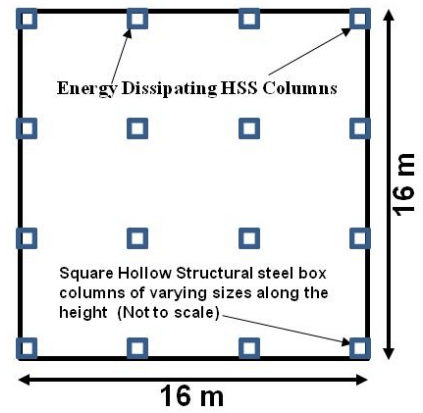


Figure 3: Building Plan View

Table 2: Member sizes and Floor Energy Dissipation

Story Level	Design:A		Design:B	
	Member Size Sides x thickness	Energy/ Floor (kN.m)	Member Size Sides x thickness	Energy/ Floor (kN.m)
10 - 9	127x127x4.8	13783	152x152x4.8	14634
8 - 7	152x152x6.4	23637	152x152x9.5	45656
6 - 5	178x178x8.0	36138	203x203x9.5	50278
4 - 3	203x203x8.0	37757	254x254x8.0	40685
2 - 1	254x254x8.0	40685	305x305x9.5	57586

Table 2 shows the resulting column sizes and the corresponding energy dissipation potential of each floor consisting of sixteen columns. Only the square HSS members were selected for this study. The sizes of the columns, when the building is subject to gravity loading, and moderate to severe lateral loading were considered and are shown in Table 2 as Design:A and Design:B, respectively. Each story uses the same size columns, and each column section spans over two story heights. Obviously, based on factored loads, a designer can choose any one of many possible HSS members available for this building. A different designer might have selected an entirely different set of columns than the steel sections selected for this study. The resulting energy dissipation potential would be different. From Table 2 and from equation 1, it is evident that the thickness of the hollow section significantly influences the energy dissipation. Thus, given the same axial capacity requirement, a designer should choose a thicker HSS section. For the analysis results presented below, the building columns were further subdivided into two categories, namely, full axial crush energy dissipation ($\rho = 1$), and partial energy dissipation with only 50% effectiveness of the symmetric crush mode collapse case ($\rho = 0.5$). These latter cases take account of the likelihood that the column failure is due to a combination of crushing and plastic bending. The energy dissipating capacities corresponding to the $\rho = 0.5$ case would be 50% of the energy values shown in Table 2.

5. Results

Assume a catastrophic event occurring at story n causes its columns to fail, and as such, roof and floor levels above story n come crashing down in freefall for a distance $h_n = 3.75$ m, providing an initial velocity of 8.58 m/s. Calculations employing the equations listed in Section 3 were performed for total loss of strength of the columns in all 10 stories for the four design and energy dissipation combinations discussed earlier. Figure 4 indicates the velocity differences experienced by the roof for a given design of the structure when a particular story is suddenly degraded. This case corresponds to Design:A with partial energy dissipation ($\rho = 0.5$).

For example, removal of story 1 results in a smooth increase in velocity throughout the progressive crush-up collapse event. On the other hand, a sudden localized collapse of story 10 results in saw-tooth motion due to the transfer of momentum story-by-story as the upper block crushes downwards until total collapse occurs. Meanwhile, sudden degradation of story 5 is a mix of downward crushing with consequent momentum exchanges, followed by crush-up failure to the roof without changes of momentum.

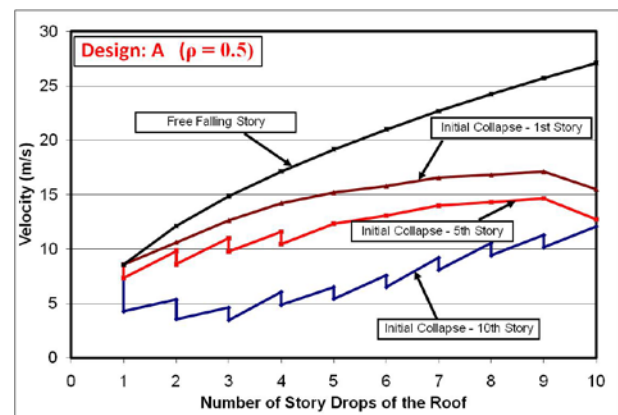


Figure 4: Velocity of Roof During Collapse

To illustrate such motions with respect to time, both designs with $\rho = 1.0$ and 0.5 were considered. Figure 5 shows the results which are very similar to Figure 4 but have the advantage of indicating the times of incremental and final collapse. First let's focus on the results corresponding to partial energy dissipation (Figures 5[B] and 5[D]). Removal of the columns in story 10, and the subsequent progression of collapse story-by-story, resulted in longer total time of collapse than when bottom story strength is suddenly withdrawn. The reason for such a difference is that crush-down involves momentum transfers as stories impact with one another. Contrast this case with the crush-up scenario, in which the bottom story is removed and the 2nd story columns must offer resistance without the benefit of momentum transfer. As such, they are subjected to an initial velocity of 8.58 m/s. The large mass, (mass of nine floors above), together with a similarly large potential energy term overpowers that story's energy dissipation ability, resulting in an ever-increasing velocity until collapse. The plot for this scenario is a smooth curve, as noted in the figure. Initial collapse at 5th story involves crush-down followed by crush-up. As expected, the collapse times and final velocities fall in between these two extremes (i.e. initial collapse 10th story and initial collapse 1st story). Of particular interest is a comparison with freefall time of the roof striking

the debris pile at ground level. The assumed 37.5 m fall would take place in 2.765 seconds. Figure 5[A] shows velocity- time plots for the Design:A cases (lightest column design) with full energy dissipation ($\rho = 1.0$) in which stories 1, 5 and 10 suddenly degrade and fail. Note that the time in these plots is either complete collapse or ‘time to arrest’ (reflected by zero velocity), denoting partial collapse of the structure only. Removal of story 10 will result in arrest during crush of the 8th story after only 2.979 sec. In the case of initial collapse in story 5, the motion is arrested in story 10, indicating crush-down failure to the ground level and then an incomplete crush-up failure. Complete collapse of the building ensues when 1st story fails in Design:A- $(\rho = 1.0)$ building. Design:B with full energy dissipation cases (Figure 5[D]) resulted in arrested collapse. For this case, initial collapses at 1st story and 5th story were arrested in floor 7, whereas initial collapse at 10th story causes crush down collapse until floor 8 where it was arrested.

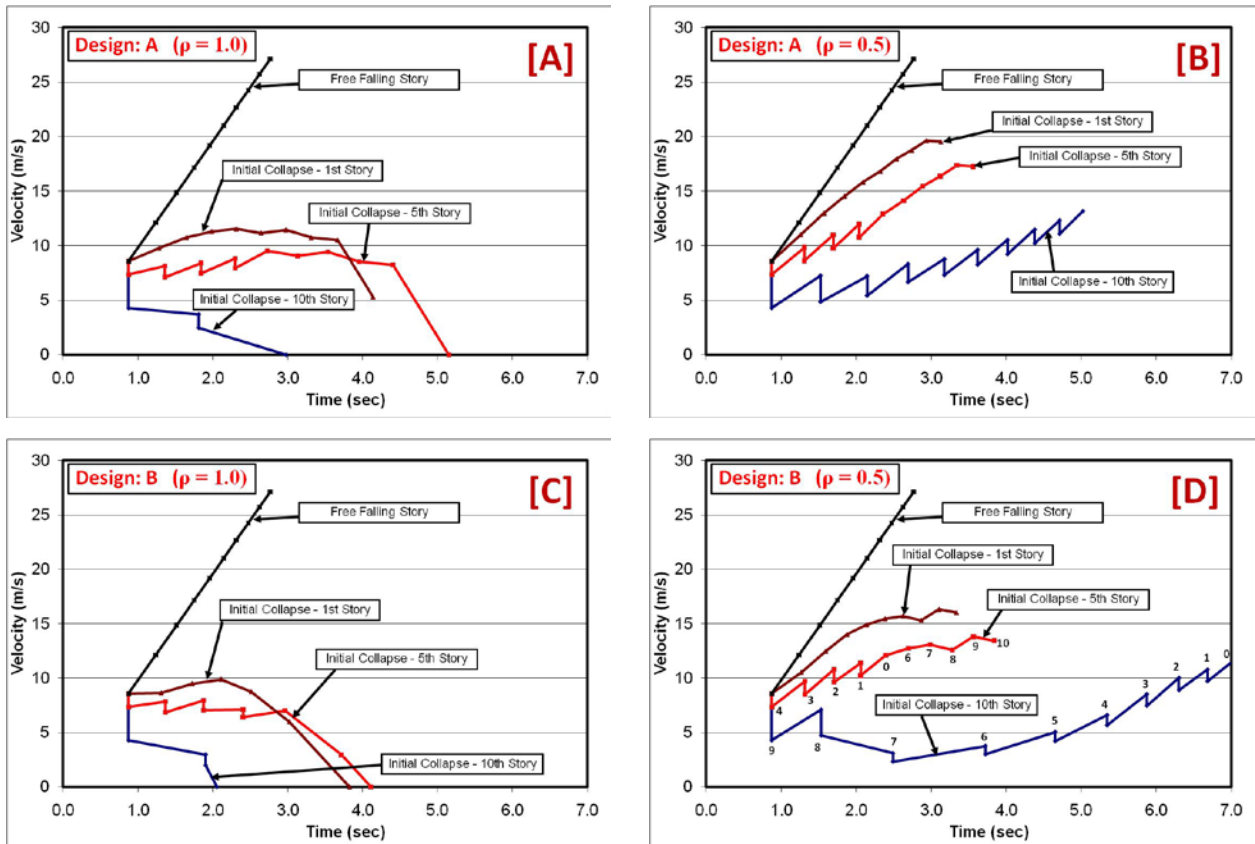


Figure 5: Motion History for the four design and energy dissipation combinations

Table: 3 Impact of energy dissipating elements on the total collapse/arrest times of a 10-story building

Initial Collapse Storey	Design: A		Design: B	
	$\rho = 1.0$	$\rho = 0.5$	$\rho = 1.0$	$\rho = 0.5$
	(Seconds)	(Seconds)	(Seconds)	(Seconds)
10	2.979 (8)*	5.020	2.056 (8)*	7.034
9	10.313 (10)*	4.532	1.307 (8)*	6.068
8	6.820 (10)*	4.158	1.736 (7)*	4.755
7	6.094 (10)*	3.953	2.533 (5)*	4.340
6	5.406 (10)*	3.715	5.048 (7)*	4.045
5	5.149 (10)*	3.559	4.109 (7)*	3.838
4	4.964 (10)*	3.421	4.001 (6)*	3.720
3	4.646	3.307	4.026 (7)*	3.595
2	4.310	3.201	3.864 (7)*	3.419
1	4.142	3.125	3.823 (7)*	3.334

* indicates partial collapse and the number within bracket shows the story which arrested the progressive collapse.

It is useful to compare the influence of the various design cases on total collapse times. Table 3 summarizes such results. The higher the story that degrades to a state of localized failure, the longer will be the structure's collapse time. For the light column cases (Design: A), it was found that 1,2, and 3rd story initial collapse led to total collapse, whereas 4 through 9 story initial collapses led to crush-down followed by crush-up failure which were arrested at the 10th story. It appears that the energy absorption of 10th story columns is considerably higher than the kinetic and the potential energies exerted by the 10th floor mass. For Design: B, all cases with full energy dissipation ($\rho = 1.0$) resulted in arrested motion in stories two or more remote from the one that suffered the initial sudden failure. Not surprisingly, the collapse times increase, or, the arrest time decreases as the column sizes increase. Most of the collapse scenarios show arrested collapse at floor 7 reflecting the energy absorption potential of this floor relative to the kinetic and potential energies of the floors above. Both, Designs: A and B with partial energy dissipation ($\rho = 0.5$) resulted in total collapse of the buildings. The collapse times increase with the increasing height of the initial collapse.

6. Concluding Remarks

The steel columns of a building can fail in various ways and then progress to a total or partial building collapse. Experiments on energy absorption of square Hollow Structural Section (HSS) steel columns in the short to intermediate range subjected to axial crush forces indicated considerable potential for energy absorption due to array of in and out folds of the sidewalls. The thickness of the hollow section significantly influences the energy dissipation. Thus, given the same axial capacity requirement, a designer should choose a thicker HSS section. This study derived an analytical model to study the progressive collapse of a multi-story steel building. The analytical investigation employed Newton's laws of motion and the energy dissipation potential of tubular sections to predict the velocity profiles and time of the collapse of multi-story buildings undergoing gravity induced progressive collapse. A summary of the totality of our investigation is given in Table 3. When total collapse occurs, the collapse times for the scenarios studied were found to range from 13 to 254% longer than free-fall. Decelerations following the initial story free-fall were noted in every case during crush-down scenarios. Although global collapses occurred for partial energy dissipation cases (with $\rho = 0.5$), arrested collapse were observed for most of the full energy dissipation cases. It should be mentioned that by ignoring the times during which the impulse-momentum equations are applicable (during collisions with individual stories), and the energy dissipation contributions of secondary structural and non-structural elements, that the results of our

analysis represent lower bounds on collapse times, and exclude collapse cases which may indeed only suffer partially. The results of our study also suggest that a new approach is needed in structural steel design, especially those employing square tubular columns, to have an ability to withstand global collapse under conditions which render given stories a degree of strength degradation that will cause only localized collapse.

7. References

- Abramowicz, W. and Jones, N., (1986), Dynamic Progressive Buckling of Circular and Square Tubes, Int. J. Impact Engineering, Vol. 4, No.4, pp 243-270.
- CSA, (2009), "S16-09 Design of Steel Structures", Canadian Standards Association, Mississauga, Ontario, Canada.
- Wierzbicki, T. and Abramowicz, W.,(1983), On the Crushing Mechanics of Thin-Walled Structures, J. of Applied Mechanics, ASCE, Vol.50, No.4A, pp 727-734.